

Is Increased Acetabular Cartilage or Fossa Size Associated With Pincer Femoroacetabular Impingement?

Stephanie Y. Pun MD, Andreas Hingsammer MD, Michael B. Millis MD,
Young-Jo Kim MD, PhD

Published online: 8 September 2016
© The Association of Bone and Joint Surgeons® 2016

Abstract

Background Surgical treatment for pincer femoroacetabular impingement (FAI) of the hip remains controversial, between trimming the prominent acetabular rim and reverse periacetabular osteotomy (PAO) that reorients the acetabulum. However, rim trimming may decrease articular surface size to a critical threshold where increased joint contact forces lead to joint degeneration. Therefore, knowledge of how much acetabular articular cartilage is

available for resection is important when evaluating between the two surgical options. In addition, it remains unclear whether the acetabulum rim in pincer FAI is a prominent rim because of increased cartilage size or increased fossa size.

Questions/purposes We used reformatted MR and CT data to establish linear length dimensions of the lunate cartilage and cotyloid fossa in normal, dysplastic, and deep acetabula.

Methods We reviewed the last 200 hips undergoing PAO, reverse PAO, and surgical dislocation for acetabular rim trimming at one institution. We compared MR images of symptomatic hips with acetabular dysplasia (20 hips), pincer FAI (29 hips), and CT scans of asymptomatic hips from patients who underwent CT scans for reasons other than hip pain (20 hips). These hips were chosen sequentially from the underlying pool of 200 potential subjects to identify the first 10 male and the first 10 female hips in each group that met inclusion criteria. As a result of low numbers, we included all hips that had undergone reverse PAO and met inclusion criteria. Cartilage width was measured medially from the cotyloid fossa to the lateral labrochondral junction. Cotyloid fossa linear height was measured from superior to inferior and cotyloid fossa width was measured from anterior to posterior. Superior lunate cartilage width (SLCW) and cotyloid fossa height (CFH) were measured on MR and CT oblique coronal reformats; anterior lunate cartilage width (ALCW), posterior lunate cartilage width (PLCW), and cotyloid fossa width (CFW) were measured on MR and CT oblique axial reformats. Cohorts were compared using multivariate analysis of variance with Bonferroni's adjustment for multiple comparisons.

Results Compared with control acetabula, dysplastic acetabula had smaller SLCW (2.08 ± 0.29 mm versus 2.63

One of the authors (Y-JK) reports personal fees from Smith & Nephew Arthroscopy (Andover, MA, USA) and personal fees from Orthopediatrics (Warsaw, IN, USA) outside the submitted work. All ICMJE Conflict of Interest Forms for authors and *Clinical Orthopaedics and Related Research*® editors and board members are on file with the publication and can be viewed on request. Each author certifies that his or her institution approved the human protocol for this investigation, that all investigations were conducted in conformity with ethical principles of research, and that informed consent for participation in the study was obtained. This work was performed at Boston Children's Hospital, Boston, MA, USA.

S. Y. Pun (✉)
Department of Orthopaedic Surgery, Stanford University School of Medicine, 300 Pasteur Drive, Edwards R105, Stanford, CA 94305, USA
e-mail: sypun@stanford.edu

A. Hingsammer
Department of Orthopaedics, Uniklinik Balgrist, University of Zurich, Zurich, Switzerland

A. Hingsammer
Department of Trauma Surgery, Medical University of Vienna, Vienna, Austria

M. B. Millis, Y.-J. Kim
Department of Orthopaedic Surgery, Harvard Medical School, Boston Children's Hospital, Boston, MA, USA

± 0.42 mm, mean difference = -0.55 mm; 95% confidence interval [CI] = -0.83 to -0.27 ; $p < 0.01$), ALCW (1.20 ± 0.34 mm versus 1.64 ± 0.21 mm, mean difference = -0.44 mm; 95% CI = -0.70 to -0.18 ; $p = 0.00$), CFH (2.84 ± 0.37 mm versus 3.42 ± 0.57 mm, mean difference = -0.59 mm; 95% CI = -0.96 to -0.21 ; $p < 0.01$), and CFW (1.98 ± 0.50 mm versus 2.77 ± 0.33 mm, mean difference = -0.80 mm; 95% CI = -1.16 to -0.42 ; $p < 0.0001$). Based on the results, we identified two subtypes of deep acetabula. Compared with controls, deep subtype 1 had normal CFH and CFW but increased ALCW (2.09 ± 0.42 mm versus 1.64 ± 0.21 mm; $p < 0.001$) and PLCW (2.32 ± 0.36 mm versus 2.00 ± 0.32 mm; $p = 0.04$). Compared with controls, deep subtype 2 had increased CFH (4.37 ± 0.51 mm versus 3.42 ± 0.57 mm; $p < 0.01$) and CFW (2.76 ± 0.54 mm versus 2.77 ± 0.33 mm; $p = 1.0$) but smaller SCLW (2.12 ± 0.40 mm versus 2.63 ± 0.42 mm; $p < 0.01$).

Conclusions Deep acetabula have two distinct morphologies: subtype 1 with increased anterior and posterior cartilage lengths and subtype 2 with a larger fossa in height and width and smaller superior cartilage length.

Clinical Relevance In patients with deep subtype 1 hips that have increased anterior and posterior cartilage widths, rim trimming to create an articular surface of normal size may be reasonable. However, for patients with deep subtype 2 hips that have large fossas but do not have increased cartilage widths, we propose that a reverse PAO that reorients yet preserves the size of the articular surface may be more promising. However, these theories will need to be validated in well-controlled clinical studies.

Introduction

Deep acetabula are a recognized cause of pincer femoroacetabular impingement (FAI) [8–10, 23]. Surgical treatment for pincer FAI remains controversial between rim trimming the prominent acetabular rim and reverse periacetabular osteotomy (PAO) that reorients the acetabulum (Fig. 1). One concern regarding rim trimming is that it may decrease articular surface size to a critical threshold where increased joint contact forces lead to joint degeneration. Therefore, consideration of acetabular lunate cartilage size may be important in choosing which surgical tactic to pursue, but limited data exist regarding detailed pincer acetabular morphology [27].

Cadaveric studies have looked at the overall size, topography, and orientation of the normal acetabulum [15, 16]. Previous studies using CT of human hips have measured the contours of the bony acetabulum [13], the relative coverage of the femoral head by the acetabulum in developmental dysplasia of the hip [1, 2, 5, 7], and the contact pressure between the acetabulum and the femoral head [12]. However, these studies have focused on normal and dysplastic hips and did not directly visualize the articular cartilage using MR. Steppacher and colleagues [27] used MR radial sequences to examine protrusio, deep, and retroverted acetabula, finding that retroverted acetabula had smaller cartilage surfaces than deep and protrusio acetabula. However, the measurements in these previous CT and MR studies were subject to imaging reformatting that can influence the accuracy of measurements because the measurements were obtained on either standard axial and

Fig. 1A–C (A) This AP pelvis radiograph shows an example of pincer FAI secondary to a deep acetabulum causing global overcoverage. (B) Subsequent treatment with a surgical dislocation approach revealed overgrown acetabular rim above the acetabular labrum, which was corrected with acetabular rim trimming. (C) This AP pelvis radiograph shows an example of bilateral pincer FAI secondary to acetabular retroversion. Note the presence of crossover signs, posterior wall signs, and ischial spine signs. The more symptomatic left hip was treated with a reverse PAO.

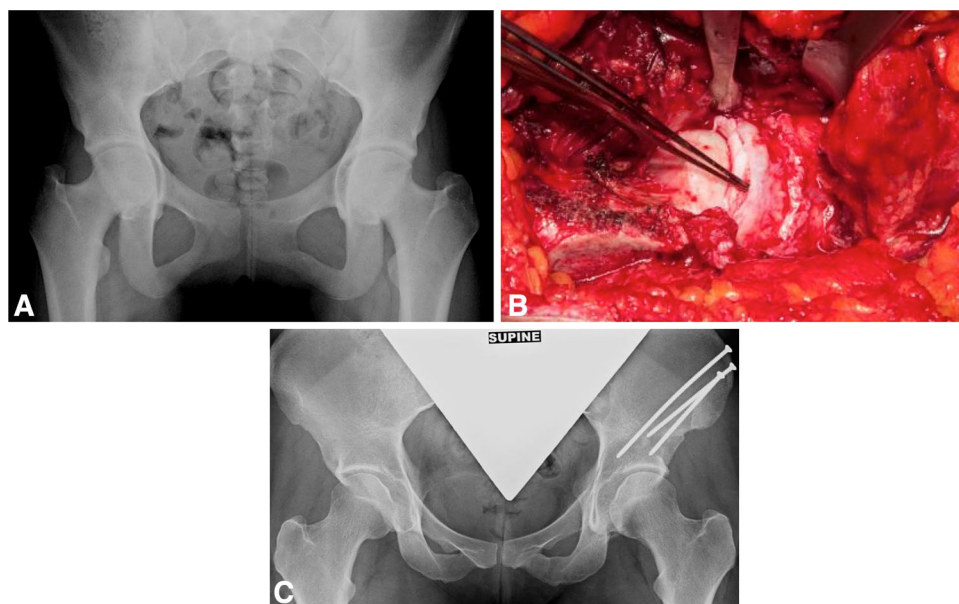


Table 1. Summary of radiographic measurements by surgical group

Group	LCEA	TA	ACEA
Control	29 ± 4	5 ± 5	
Dysplastic—PAO	9 ± 8 [†]	20 ± 6 [†]	8 ± 11
Pincer FAI—rim trim	38 ± 9*	1 ± 6	42 ± 8
Pincer FAI—reverse PAO	42 ± 10*	-3 ± 10 [†]	41 ± 11

Data are presented as mean ± SD in millimeters; * $p < 0.01$ when compared with the control group; [†] $p < 0.001$ when compared with the control group; LCEA = lateral center-edge angle; TA = Tönnis angle; ACEA = anterior center-edge angle; FAI = femoroacetabular impingement; PAO = periacetabular osteotomy.

coronal reformats, which section the acetabulum obliquely, or radial images that reference the femoral neck axis to determine the center of the acetabulum. However, it remains unclear whether the acetabulum in pincer FAI has a prominent rim because of increased cartilage size or increased fossa size.

Recent improvements in MR and CT image processing have enabled us to characterize the true dimensions of the acetabulum in planes that are parallel and orthogonal to the acetabular opening. The aim of this study was to use reformatted MR and CT data to establish the linear medial to lateral lengths of the lunatic cartilage and the linear height and linear width of the cotyloid fossa in normal, dysplastic, and deep acetabula and to determine the relative ratio of cartilage length to fossa length that comprises each type of acetabulum.

Patients and Methods

Institutional review board approval was obtained to retrospectively review the last 200 surgical cases of three types of operations at the senior authors' institution (Y-JK, MBM): PAO, reverse PAO, and surgical dislocations for acetabular rim trimming. We identified the first 10 female and 10 male patients who met inclusion criteria and had undergone PAO. We then identified the first 10 female and 10 male patients who met inclusion criteria and had undergone surgical dislocation for rim trimming. We included all patients who had undergone reverse PAO and met inclusion criteria regardless of sex because only a small number of these cases existed. We queried the study institution's radiologic database to identify pelvic CT scans that were performed for reasons other than hip pain to find 10 female and 10 male patients to form a control group. Hips that were skeletally immature, hips that had undergone prior surgery, hips that had severe incongruence between the femoral head and acetabulum, hips that were additionally treated for cam FAI, and hips that did not have adequate MR or CT imaging were excluded.

Three cohorts were established: (1) asymptomatic control hips ($n = 20$); (2) symptomatic, dysplastic hips that were treated with PAO ($n = 20$); and (3) symptomatic, deep hips that were treated with either surgical dislocation for acetabular rim trim ($n = 20$) or reverse PAO ($n = 9$) for pincer FAI. We used plain radiographs to verify that the dysplastic hips and deep hips included in each cohort met the established definition criteria (Table 1). Dysplastic acetabula were defined by a lateral center-edge angle (LCEA) less than 25° [29, 30] and a minimal Tönnis angle of 14° [21]. Deep hips were defined by LCEA greater than 38° [30]. Plain films were unavailable to assess for radiographically normal anatomy for the control cohort, but the LCEA and Tönnis angle were measurable on the CT scout views, allowing confirmation that these hips had normal lateral coverage and sourcil obliquity. There was an equal distribution of males and females in each cohort (10 males, 10 females) except for the hips that underwent reverse PAO (one male, eight females).

One observer (AH) performed the MR and CT reformatting using commercially available OsiriX open source DICOM viewing software [24] to create the oblique coronal and oblique axial reformats in the following sequence. First, the sagittal reformats were aligned along the acetabular opening on the coronal view, from the superolateral aspect of the acetabulum to the inferior aspect of the acetabulum. Second, the coronal reformats were aligned perpendicular to the transverse acetabular ligament as visualized on the sagittal view. Third, the axial reformats were aligned at the inferior quartile of the acetabulum as seen on the sagittal view. Oblique coronal and oblique axial reformats were thus created. The advantage of our method of measuring linear acetabular dimensions on reformatted MR and CT images that reference the opening of the acetabulum itself is that it allows us to inspect the acetabulum without concern for the effects of individual pelvic tilt, the patient's position in the MR scanner, and variations of proximal femoral anatomy.

The terminology for measurements performed in this study is as follows. Linear length measurements of the

Fig. 2 Schematic diagram shows the linear length measurements of lunate cartilage and cotyloid fossa assessed in this study.

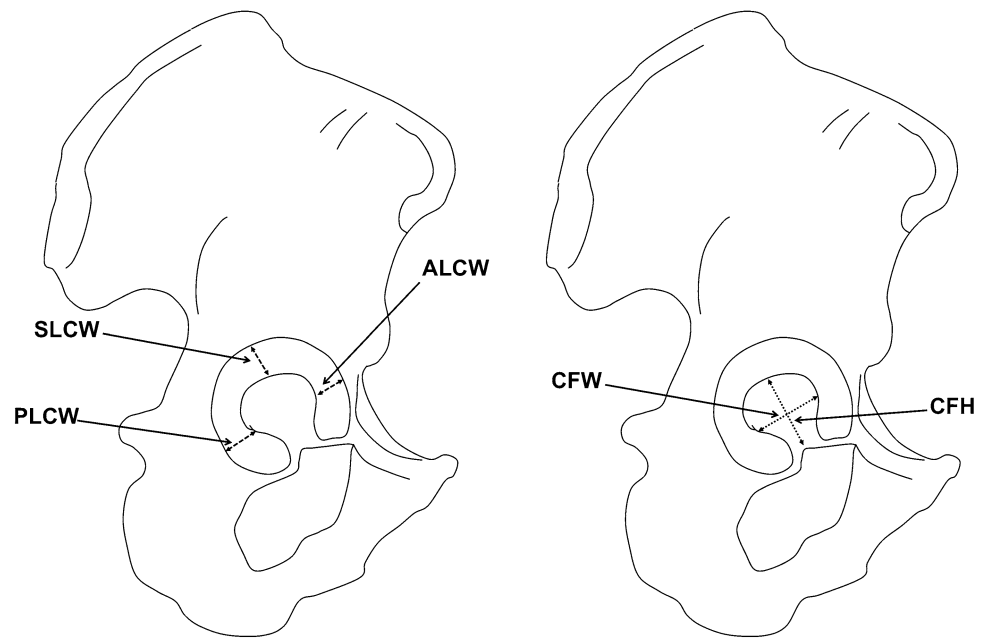
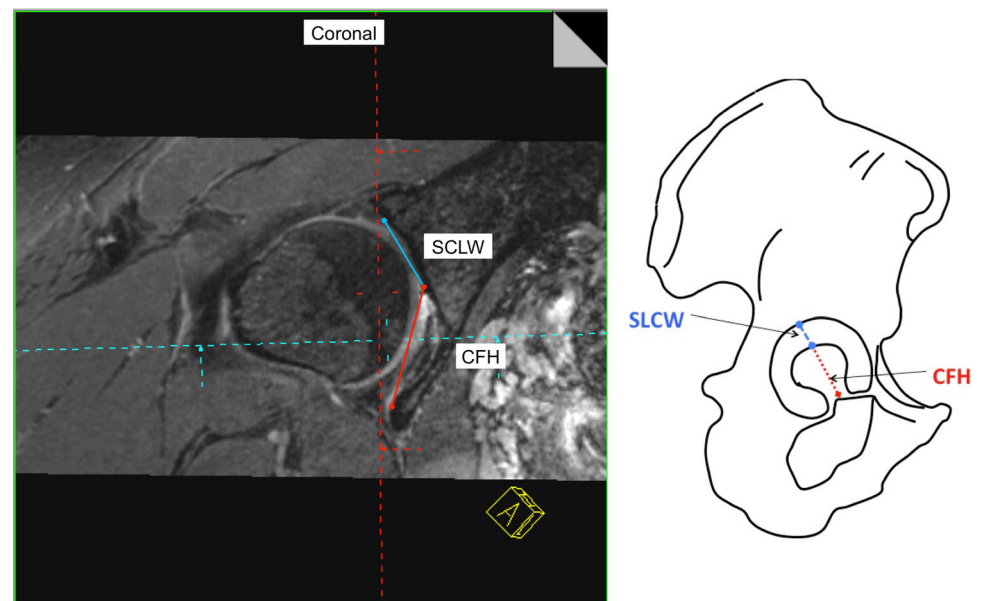


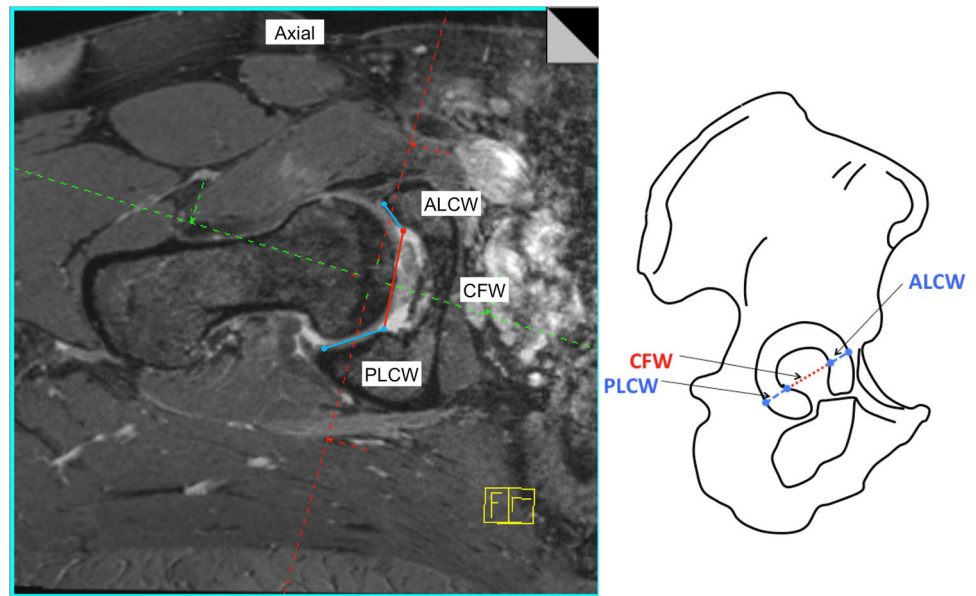
Fig. 3 Oblique coronal MR images were used to measure SLCW and CFH.



lunate cartilage are described as “width” of the cartilage surface proceeding from the medial edge of the cartilage near the fossa to the lateral edge of the cartilage at the labrochondral junction (Fig. 2). Linear measurements of the length of the cotyloid fossa are described as “width” when measuring the fossa from anterior to posterior and “height” when measuring the fossa from superior to inferior. The superior lunate cartilage width (SLCW) and the cotyloid fossa height (CFH) were measured on the oblique coronal reformat at the center of the acetabulum (Fig. 3). SLCW was measured from the medial extent of the lunate

cartilage at the top of the cotyloid fossa to the labrochondral junction (on MRI) or the lateral edge of the sourcil (on CT). CFH was measured from the top of the cotyloid fossa to the transverse acetabular ligament (MRI) or the most inferior portion of the bony fossa (CT). The anterior lunate cartilage width (ALCW), posterior lunate cartilage width (PLCW), and the cotyloid fossa width (CFW) were measured on the oblique axial reformat at the inferior quartile of the acetabulum (Fig. 4). ALCW was measured from the medial extent of the lunate cartilage adjacent to the fossa to the anterior labrochondral junction. PLCW was measured

Fig. 4 Oblique axial MR images were used to measure anterior (ALCW) and posterior (PLCW) lunate cartilage widths and CFW.



from the medial extent of the lunate cartilage adjacent to the fossa to the posterior labrochondral junction. CFW was measured from the anterior extent to the posterior extent of the fossa.

Statistical Analysis

Mean values for SLCW, ALCW, PLCW, CFH, and CFW in each of the three cohorts were calculated and then compared across the three cohorts. The ratios of lunate cartilage length to cotyloid fossa length on the oblique coronal reformats (SLCW:CFH) and ratios of lunate cartilage length to cotyloid fossa length on the oblique axial reformats ($[ALCW + PLCW]:CFW$) were calculated and averaged within each cohort and then compared across the three cohorts.

Normality of each outcome measure was assessed with the Shapiro–Wilks test. No deviation from normality was detected for any of the outcome measurements. Univariate and multivariate analysis of variance was implemented to compare across cohort groups the two oblique coronal outcome measurements (SLCW and CFH), the three oblique axial outcome measurements (ALCW, PLCW, and CFW), and two cartilage to fossa ratio measurements (SLCW:CFH and $[ALCW + PLCW]:CFW$). Orthogonal contrasts were used to compare measurements for the dysplastic and deep groups with the control group for each outcome based on a priori hypotheses. Post hoc analysis was conducted to assess the mean differences between cohorts using Dunnett's adjustment for multiple comparisons. Additional comparisons between noncontrol patient groups were conducted using Bonferroni's adjustment for

multiple comparisons. Probability values < 0.05 were considered significant. Analysis was performed using SAS Version 9.3 (SAS Institute Inc, Cary, NC, USA).

Results

Lunate cartilage widths and cotyloid fossa width and height differed among the three groups (Table 2). Based on the results, we identified four different types of acetabula: control, dysplastic, and two subtypes of deep acetabula that we have termed subtype 1 and subtype 2 (Figs. 5, 6).

Superior Lunate Cartilage Width

Dysplastic hips had lower SLCW measurements compared with control hips (2.08 ± 0.29 mm versus 2.63 ± 0.42 mm, mean difference = -0.55 mm; 95% confidence interval [CI] = -0.83 to -0.27 ; $p < 0.01$) (Table 3). Deep subtype 2 hips also had lower SLCW measurements compared with control hips (2.12 ± 0.40 mm versus 2.63 ± 0.42 mm, mean difference = -0.51 mm; 95% CI = -0.86 to -0.16 ; $p < 0.01$). There was no difference in SLCW measurements between deep subtype 1 hips and control hips (2.86 ± 0.32 mm versus 2.63 ± 0.42 mm, mean difference = 0.23 mm; 95% CI = -0.05 to 0.50 ; $p = 0.15$).

Anterior Lunate Cartilage Width

Dysplastic hips had lower ALCW measurements compared with control hips (1.20 ± 0.34 mm versus 1.64 ± 0.21 mm,

Table 2. Summary measurements by group

	Coronal view		Axial view			Coronal ratio	Axial ratio
	SLCW	CFH	ALCW	PLCW	CFW		
All	2.47 ± 0.48	3.39 ± 0.67	1.62 ± 0.48	1.98 ± 0.46	2.61 ± 0.65	0.75 ± 0.20	1.45 ± 0.43
Control	2.63 ± 0.42	3.42 ± 0.57	1.64 ± 0.21	2.00 ± 0.32	2.77 ± 0.33	0.79 ± 0.21	1.33 ± 0.18
Dysplastic	2.08 ± 0.29	2.84 ± 0.37	1.20 ± 0.34	1.74 ± 0.38	1.98 ± 0.50	0.74 ± 0.14	1.55 ± 0.42
Subtype 1	2.86 ± 0.32	3.48 ± 0.50	2.09 ± 0.42	2.32 ± 0.36	2.76 ± 0.54	0.84 ± 0.17	1.66 ± 0.48
Subtype 2	2.12 ± 0.40	4.37 ± 0.51	1.47 ± 0.33	1.69 ± 0.64	3.40 ± 0.45	0.49 ± 0.12	0.94 ± 0.29

Data are presented as mean ± SD in millimeters; bold entries indicate significant difference from the control group at the 5% level; SLCW = superior lunate cartilage width; ALCW = anterior lunate cartilage width; PLCW = posterior lunate cartilage width; CFH = cotyloid fossa height; CFW = cotyloid fossa width; LC = sum of ALCW and PLCW measurements.

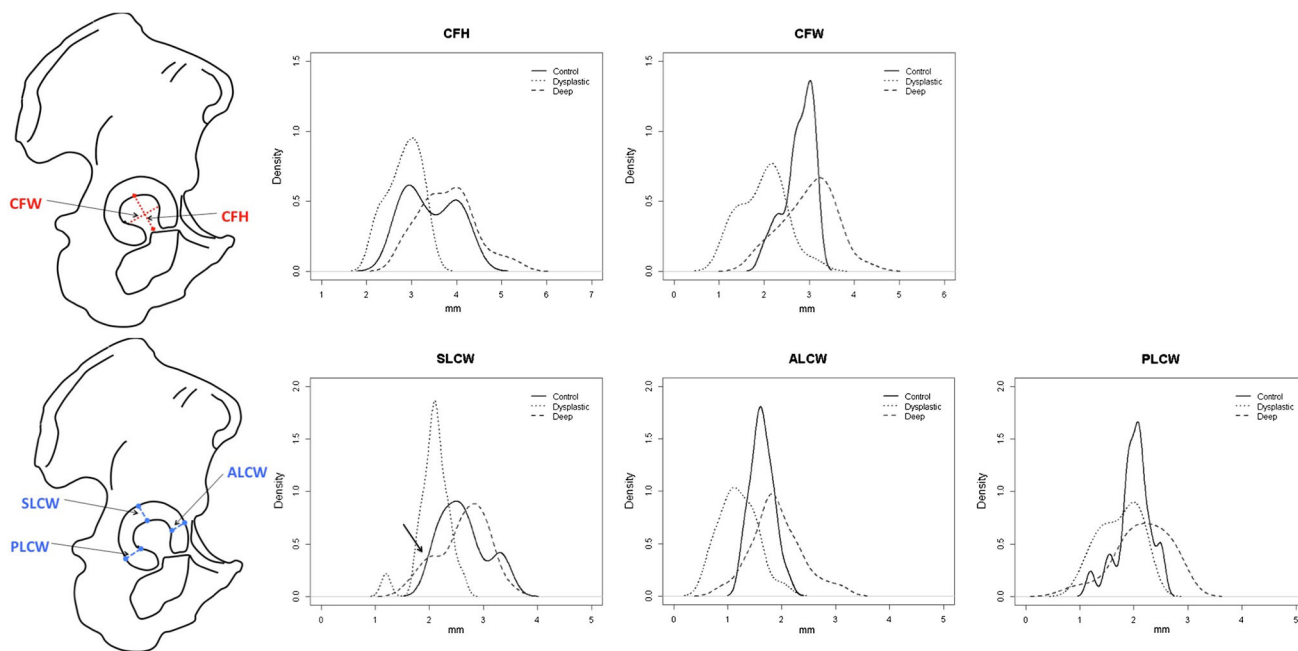


Fig. 5 Distribution plots represent control, dysplastic, and deep acetabula cartilage and fossa lengths. Dysplastic hips had overall decreased cartilage and fossa lengths compared with both control and deep acetabula. Distribution plot of SLCW shows two peaks

representing the two subtypes of deep acetabula. There was no difference in SLCW between subtype 1 and the control. Subtype 2 (arrow) has decreased SLCW compared with the control.

mean difference = -0.44 mm; 95% CI = -0.70 to -0.18; $p < 0.001$). In contrast, deep subtype 1 hips had higher ALCW measurements compared with control hips (2.09 ± 0.42 mm versus 1.64 ± 0.21 mm, mean difference = 0.45 mm; 95% CI = 0.19–0.71; $p < 0.001$). There was no difference in ALCW measurements between deep subtype 2 hips and control hips (1.47 ± 0.33 mm versus 1.64 ± 0.21 mm, mean difference = -0.17 mm, 95% CI = -0.52 to 0.17; $p = 0.67$).

± 0.32 mm, mean difference = -0.27 mm, 95% CI = -0.57 to 0.04; $p = 0.11$). Deep subtype 1 hips had higher PLCW measurements compared with control hips (2.32 ± 0.36 mm versus 2.00 ± 0.32 mm, mean difference = 0.32 mm; 95% CI = 0.01–0.62; $p = 0.04$). There was no difference in PLCW measurements between deep subtype 2 hips and control hips (1.69 ± 0.64 mm versus 2.00 ± 0.32 mm, mean difference = -0.31 mm, 95% CI = -0.71 to 0.10; $p = 0.21$).

Posterior Lunate Cartilage Width

There was no difference in PLCW measurements between dysplastic hips and control hips (1.74 ± 0.38 mm versus 2.00

Cotyloid Fossa Height

Dysplastic hips had lower CFH measurements compared with control hips (2.84 ± 0.37 mm versus 3.42 ± 0.57 mm,

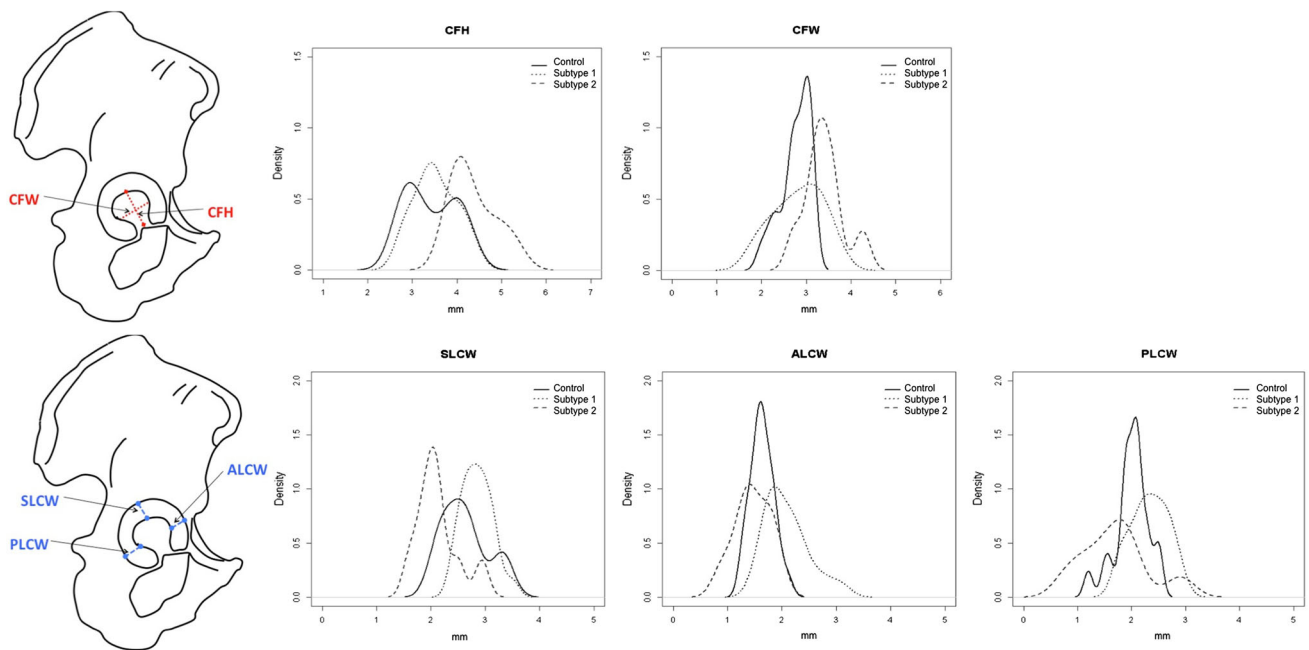


Fig. 6 Distribution plots represent cartilage and fossa lengths in subtype 1 and subtype 2 deep acetabula. Subtype 1 (short dashed line) distribution plots show normal fossa height and width and increased

mean difference = -0.59 mm; 95% CI = -0.96 to -0.21 ; $p < 0.01$). In contrast, deep subtype 2 hips had higher CFH measurements compared with control hips (4.37 ± 0.51 mm versus 3.42 ± 0.57 mm, mean difference = 0.95 mm; 95% CI = 0.47 – 1.43 ; $p < 0.01$). There was no difference in CFH measurements between deep subtype 1 hips and control hips (3.48 ± 0.50 mm versus 3.42 ± 0.57 mm, mean difference = 0.06 mm; 95% CI = -0.32 to 0.43 ; $p = 1.0$).

Cotyloid Fossa Width

Dysplastic hips had lower CFW measurements compared with control hips (1.98 ± 0.50 mm versus 2.77 ± 0.33 mm, mean difference = -0.80 mm; 95% CI = -1.16 to -0.42 ; $p < 0.001$). In contrast, deep subtype 2 hips had higher CFW measurements compared with control hips (3.40 ± 0.45 mm versus 2.77 ± 0.33 mm, mean difference = 0.63 mm; 95% CI = 0.15 – 1.11 ; $p = 0.01$). There was no difference in CFW measurements between deep subtype 1 hips and control hips (2.76 ± 0.54 mm versus 2.77 ± 0.33 mm, mean difference = -0.01 mm, 95% CI = -0.37 to 0.35 ; $p = 1.0$).

Dysplastic Hips

As shown previously, dysplastic hips had lower SLCW, ALCW, CFH, and CFW values when compared with control hips. Overall, SLCW in dysplastic hips was 21% lower than in control hips. There was no difference in the ratio of

anterior and posterior cartilage lengths. Subtype 2 (long dashed line) distribution plots show increased fossa height and width and decreased superior lunate cartilage length.

SLCW to CFH in dysplastic hips compared with control hips (0.74 ± 0.14 versus 0.79 ± 0.21 , mean difference = -0.05 ; 95% CI = -0.18 to 0.08 ; $p = 1.0$) (Table 4). Likewise, there was no difference in the ratio of (ALCW + PLCW) to CFW between dysplastic hips and control hips (1.55 ± 0.42 versus 1.33 ± 0.18 , mean difference = 0.22 ; 95% CI = -0.07 to 0.51 ; $p = 0.19$). Thus, when compared with control hips, dysplastic hips had proportionally lower cartilage lengths and fossa dimensions.

Deep Subtype 1 Hips

There was no difference in the ratio of SLCW to CFH in deep subtype 1 hips compared with control hips (0.84 ± 0.17 versus 0.79 ± 0.21 , mean difference = 0.05 ; 95% CI = -0.08 to 0.18 ; $p = 1.0$). However, there were higher cartilage to fossa ratios in deep subtype 1 hips when comparing the ratio of (ALCW + PLCW) to CFW between deep subtype 1 hips and control hips (1.66 ± 0.48 versus 1.33 ± 0.18 , mean difference = 0.34 ; 95% CI = 0.05 – 0.63 ; $p = 0.02$). Thus, when compared with control hips, deep subtype 1 hips had disproportionately increased anterior and posterior cartilage widths.

Deep Subtype 2 Hips

Overall, SLCW in deep subtype 2 hips was 19% lower than in control hips. There were lower cartilage to fossa ratios in

Table 3. Multiple comparisons by group (control, dysplastic, subtype 1, and subtype 2)

Comparison	Mean	95% confidence interval for the mean	Mean difference*	95% confidence interval for the mean difference	p value
SLCW					
Control	2.63	(2.47, 2.79)			
Dysplastic	2.08	(1.92, 2.24)	-0.55	(-0.83, -0.27)	< 0.001
Subtype 1	2.86	(2.70, 3.01)	0.23	(-0.05, 0.50)	0.15
Subtype 2	2.12	(1.88, 2.36)	-0.51	(-0.86, -0.16)	< 0.001
ALCW					
Control	1.64	(1.49, 1.78)			
Dysplastic	1.20	(1.05, 1.34)	-0.44	(-0.70, -0.18)	< 0.001
Subtype 1	2.09	(1.94, 2.23)	0.45	(0.19, 0.71)	< 0.001
Subtype 2	1.46	(1.23, 1.70)	-0.17	(-0.52, 0.17)	0.67
PLCW					
Control	2.00	(1.82, 2.18)			
Dysplastic	1.74	(1.56, 1.91)	-0.27	(-0.57, 0.04)	0.11
Subtype 1	2.32	(2.14, 2.49)	0.32	(0.01, 0.62)	0.04
Subtype 2	1.69	(1.42, 1.97)	-0.31	(-0.71, 0.10)	0.21
CFH					
Control	3.42	(3.20, 3.64)			
Dysplastic	2.84	(2.62, 3.05)	-0.59	(-0.96, -0.21)	< 0.001
Subtype 1	3.48	(3.26, 3.69)	0.06	(-0.32, 0.43)	1.00
Subtype 2	4.37	(4.05, 4.70)	0.95	(0.47, 1.43)	< 0.001
CFW					
Control	2.77	(2.56, 2.98)			
Dysplastic	1.98	(1.77, 2.18)	-0.80	(-1.16, -0.43)	< 0.001
Subtype 1	2.76	(2.55, 2.97)	-0.01	(-0.37, 0.35)	1.00
Subtype 2	3.40	(3.07, 3.73)	0.63	(0.15, 1.11)	0.01

Data are presented as mean \pm SD in millimeters; *a negative mean difference implies that the group measure was lower than the control measure; bold entries indicate significant difference from the control group at the 5% level; SLCW = superior lunate cartilage width; ALCW = anterior lunate cartilage width; PLCW = posterior lunate cartilage width; CFH = cotyloid fossa height; CFW = cotyloid fossa width; LC = the sum of ALCW and PLCW measurements.

Table 4. Coronal and axial cartilage to fossa ratio multiple comparisons by group (control, dysplastic, subtype 1, and subtype 2)

	Mean	95% confidence interval for the mean	Mean difference*	95% confidence interval for the mean difference	p value
SLCW:CFH					
Control	0.79	(0.72, 0.87)			
Dysplastic	0.74	(0.67, 0.82)	-0.05	(-0.18, 0.08)	1.00
Subtype1	0.84	(0.77, 0.92)	0.05	(-0.08, 0.18)	1.00
Subtype2	0.49	(0.38, 0.61)	-0.30	(-0.46, -0.13)	< 0.001
LC:CFW					
Control	1.33	(1.16, 1.49)			
Dysplastic	1.55	(1.38, 1.71)	0.22	(-0.07, 0.51)	0.19
Subtype1	1.66	(1.50, 1.83)	0.34	(0.05, 0.63)	0.02
Subtype2	0.94	(0.68, 1.20)	-0.38	(-0.77, 0.00)	0.05

*A negative mean difference implies that the group measure was lower than the control measure; bold entries indicate significant difference from the control group at the 5% level; SLCW = superior lunate cartilage width; ALCW = anterior lunate cartilage width; PLCW = posterior lunate cartilage width; CFH = cotyloid fossa height; CFW = cotyloid fossa width; LC = the sum of ALCW and PLCW measurements.

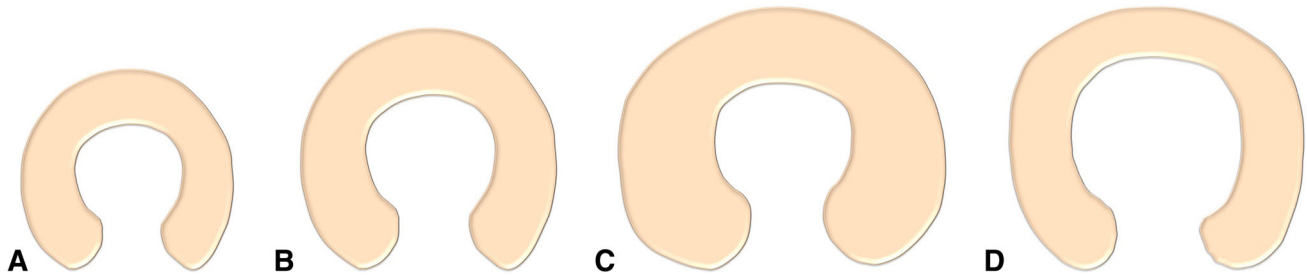


Fig. 7A–D Schematic drawing depicts four acetabula morphologic types. **(A)** Dysplastic acetabula: overall smaller cartilage and fossa lengths than controls. **(B)** Control acetabula. **(C)** Deep subtype 1 acetabula: larger anterior and posterior cartilage lengths but normal

fossa height and width. **(D)** Deep subtype 2 acetabula: smaller superior cartilage length, normal anterior and posterior cartilage sizes, and larger fossa height and width.

deep subtype 2 hips when comparing the ratio of SLCW to CFH between deep subtype 2 hips and control hips (0.49 ± 0.12 versus 0.79 ± 0.21 , mean difference = -0.30 ; 95% CI = -0.46 to -0.13 ; $p < 0.001$). There was no difference detected in the ratio of (ALCW + PLCW) to CFW between deep subtype 2 hips and control hips (0.94 ± 0.29 versus 1.33 ± 0.18 , mean difference = -0.38 ; 95% CI = -0.77 to 0.00 ; $p = 0.05$). Thus, when compared with control hips, deep subtype 2 hips had disproportionally increased fossa height and decreased superior cartilage width.

Discussion

Pincer FAI is associated with deep acetabula that overcover the femoral head. Available research on the anatomy of deep acetabula has mostly focused on parameters quantifying the amount of overcoverage; less attention has been paid to the relative contributions of the size of the lunate cartilage and the size of the cotyloid fossa toward the formation of a deep acetabulum. The aim of this study was to therefore quantify the lunate cartilage and fossa dimensions of normal, dysplastic, and deep acetabula. We identified four different morphologic types of acetabula (Fig. 7). Dysplastic acetabula are overall smaller than control and deep acetabula with proportionally smaller lunate cartilage and cotyloid fossa dimensions. Deep acetabula are differentiated into two subtypes. Subtype 1 of deep acetabula is characterized by disproportionally larger anterior and posterior cartilage widths but normal fossa dimensions, whereas subtype 2 of deep acetabula is defined by a disproportionally larger fossa height and width but smaller superior cartilage width.

There are limitations to our study. First, this was a retrospective study with the possibility of selection bias between groups. Pincer FAI hips included had already been treated with either acetabular rim trimming or a reverse PAO based on clinical judgment of whether the hip had focal overcoverage and a flat sourcil (rim trimming) or

global overcoverage with a high fossa and downsloping sourcil (reverse PAO). However, such selection bias did not affect the absolute acetabular dimensions measured in each hip. Second, we analyzed a limited number of MR images per hip. We chose to only include representative measurements of the lunate cartilage and cotyloid fossa in areas that we believed represented the most clinically relevant areas of the acetabulum; the superior aspect because of its role in weightbearing [11, 31] and the anterior and posterior acetabular rims because of their involvement in pincer impingement [3, 28]. Third, although linear length measurements serve to quantify dimensions of cartilage and fossa and allow comparison between different types of acetabula, they are affected by the radius of curvature of the lunate surface and fossa, so the length measurements in hips with a smaller radius of curvature may underestimate the true size of the curved lunate surface and fossa. Fourth, our sample size was relatively small so it may not reflect the heterogeneity of hip morphology in the general population. Fifth, our measurements have not been validated in cadaveric models, which may be an interesting comparison to in vivo imaging studies; however, in this study of young adult hips, an MR study was more feasible than a cadaveric study and in vivo MR images may arguably better demonstrate the lunate cartilage structure compared with a cadaveric specimen whose tissue structure has been changed by preservation and desiccation. Sixth, we did not analyze the differences between male and female hips. In general, male acetabula are larger than female acetabula. Although we tried to control for the effects of sex by including even numbers of male and female subjects in all groups except for the deep acetabula group (19 female hips and 11 male hips), sex differences in the deep acetabula group may have caused the lunate cartilage measurements to be overall lower. However, despite the decreased size of the lunate cartilage in deep subtype 2 acetabula, there was also an increased size of the cotyloid fossa, suggesting that this acetabular morphology is less attributable to sex-related acetabular size differences and more attributable to a

uniquely disproportionate ratio of lunate cartilage to cotyloid fossa in this deep acetabula subtype.

Our results for lunate cartilage and cotyloid fossa size compare well with the work of others. We found that dysplastic hips are globally deficient in both cartilage and fossa dimensions. A previous three-dimensional CT study described a volumetric decrease of 18% to 19% in dysplastic hips compared with normal hips [5]. Another CT-based study reported a 26% decrease in contact area in dysplastic hips compared with normal hips [12]. Most recently, Steppacher et al. [27] found a 16% decrease in lunate cartilage surface area in dysplastic hips compared with normal hips. We found a comparable 21% reduction of superior lunate cartilage width in dysplastic acetabula compared with control acetabula.

Interestingly, we also found a 19% reduction in superior lunate cartilage width in deep subtype 2 acetabula, akin to the reduction in superior cartilage width that was observed in dysplastic acetabula. This finding is in agreement with previously published data showing that certain types of deep acetabula have decreased lunate cartilage surface area compared with normal hips [27]. Thus, our deep subtype 2 acetabula have similar characteristics to the retroverted acetabula described by Steppacher and colleagues in that our deep subtype 2 was also observed to have smaller lunate cartilage size and larger cotyloid fossa size. In comparison, our deep subtype 1 acetabula are similar to the protrusio acetabula that they described, which is characterized by increased lunate cartilage widths and normal to increased cotyloid fossa size [27].

Our findings have several clinical implications. Our results demonstrate that pincer FAI from deep acetabula causing femoral head overcoverage may be the result of either a larger lunate cartilage surface, demonstrated in our deep subtype 1, or a larger cotyloid fossa, exemplified in our deep subtype 2. These distinct subtypes of pincer acetabula implicate that potentially different treatment options could be considered depending on the individual morphology of the acetabulum. Deep subtype 1 acetabula owe their depth to disproportionately larger anterior and posterior lunate cartilage surfaces. Thus, in patients with a deep subtype 1 hip, an acetabular rim trim to decrease the prominence of the acetabular rim and to reach a more normal lunate cartilage surface size would appear to be a reasonable treatment choice. However, future studies will need to test these suggestions.

In contrast, deep subtype 2 acetabula owe their depth to a disproportionately larger cotyloid fossa rather than an abnormally large lunate cartilage surface. A large cotyloid fossa is often seen in hips with downsloping acetabular sourcils such as in protrusio acetabula and “medial dysplasia,” where increased contact stress is concentrated at the medial aspect of the sourcil, over time resulting in medial osteoarthritis [17]. This acetabular morphology causes pincer-type impingement

laterally and static overload of the joint medially. Although acetabular rim trimming can decrease lateral impingement, decreasing the size of the articular surface can actually exacerbate the medial overload of the acetabular sourcil in these pincer variants and potentially accelerate the development of medial osteoarthritis of the hip [17].

The smaller articular surface seen in subtype 2 deep acetabula also implies higher peak contact forces and stresses on the articular cartilage. We know from mechanical and modeling studies of dysplastic hips that the higher peak contact forces and stresses on articular cartilage from a smaller contact area contribute to early joint degeneration [12, 18–20, 31]. Iatrogenic creation of a smaller articular surface with excessive acetabular rim trimming during surgical dislocation procedures is associated with poorer clinical and radiographic outcomes at both 5- and 10-year followup [25, 26]. Femoral head undercoverage from excessive rim trimming leads to more rapid joint deterioration than inadequately treated pincer impingement [25]. Thus, acetabular rim trimming in deep subtype 2 hips risks decreasing the acetabular articular surface to a precarious threshold that would elevate the joint contact forces and stresses to an unfavorable level.

The clinical challenge is to determine the safe extent of rim trimming. It is suggested through in vivo and cadaveric studies that each 1 mm of rim resection results in 1° to 2° decreases in lateral and anterior center-edge angles [6, 14, 22]. However, cadaveric studies also show that rim resection of 4 mm increases the contact pressure within the hip [4] and that rim resection of as little as 3 mm can cause instability and subluxation of the hip [6]. Thus, for patients with deep subtype 2 hips with high center-edge angles that require more than a few degrees of correction, and that have high fossas and downsloping sourcils, an acetabular reorientation procedure such as a reverse PAO may be a promising alternative treatment to alleviate impingement while preserving the size of the articular surface. However, these theories will need to be validated in well-controlled clinical studies. Future studies might examine the contact stress within each of these acetabular morphologies and focus on the clinical outcomes of different treatment options for both subtype 1 and subtype 2 deep acetabula. Understanding the relative proportions of lunate cartilage to fossa in deep acetabula variants will help to determine appropriate surgical intervention for pincer impingement.

Acknowledgments We thank Patricia Miller for her assistance with statistical analysis of data.

References

1. Anda S, Svenningsen S, Dale LG, Benum P. The acetabular sector angle of the adult hip determined by computed tomography. *Acta Radiol Diagn (Stockh)*. 1986;27:443–447.

2. Anda S, Terjesen T, Kvistad KA, Svenningsen S. Acetabular angles and femoral anteversion in dysplastic hips in adults: CT investigation. *J Comput Assist Tomogr.* 1991;15:115–120.
3. Beck M, Kalhor M, Leunig M, Ganz R. Hip morphology influences the pattern of damage to the acetabular cartilage: femoroacetabular impingement as a cause of early osteoarthritis of the hip. *J Bone Joint Surg Br.* 2005;87:1012–1018.
4. Bhatia S, Lee S, Shewman E, Mather RC, Salata MJ, Bush-Joseph CA, Nho SJ. Effects of acetabular rim trimming on hip joint contact pressures: how much is too much? *Am J Sports Med.* 2015;43:2138–2145.
5. van Bosse H, Wedge JH, Babyn P. How are dysplastic hips different? A three-dimensional CT study. *Clin Orthop Relat Res.* 2015;473:1712–1723.
6. Colvin AC, Koehler SM, Bird J. Can the change in center-edge angle during pincer trimming be reliably predicted? *Clin Orthop Relat Res.* 2011;469:1071–1074.
7. Dandachli W, Kannan V, Richards R, Shah Z, Hall-Craggs M, Witt J. Analysis of cover of the femoral head in normal and dysplastic hips: new CT-based technique. *J Bone Joint Surg Br.* 2008;90:1428–1434.
8. Ganz R, Leunig M, Leunig-Ganz K, Harris WH. The etiology of osteoarthritis of the hip: an integrated mechanical concept. *Clin Orthop Relat Res.* 2008;466:264–272.
9. Ganz R, Parvizi J, Beck M, Leunig M, Nötzli H, Siebenrock KA. Femoroacetabular impingement: a cause for osteoarthritis of the hip. *Clin Orthop Relat Res.* 2003;417:112–120.
10. Giori NJ, Trousdale RT. Acetabular retroversion is associated with osteoarthritis of the hip. *Clin Orthop Relat Res.* 2003;417:263–269.
11. Harris MD, Anderson AE, Henak CR, Ellis BJ, Peters CL, Weiss JA. Finite element prediction of cartilage contact stresses in normal human hips. *J Orthop Res.* 2012;30:1133–1139.
12. Hipp JA, Sugano N, Millis MB, Murphy SB. Planning acetabular redirection osteotomies based on joint contact pressures. *Clin Orthop Relat Res.* 1999;364:134–143.
13. Klaue K, Wallin A, Ganz R. CT evaluation of coverage and congruency of the hip prior to osteotomy. *Clin Orthop Relat Res.* 1988;232:15–25.
14. Kling S, Karns MR, Gebhart J, Kosmas C, Robbin M, Nho SJ, Bedi A, Salata MJ. The effect of acetabular rim recession on anterior acetabular coverage: a cadaveric study using the false-profile radiograph. *Am J Sports Med.* 2015;43:957–964.
15. Köhnllein W, Ganz R, Impellizzeri FM, Leunig M. Acetabular morphology: implications for joint-preserving surgery. *Clin Orthop Relat Res.* 2009;467:682–691.
16. Krebs V, Incavo SJ, Shields WH. The anatomy of the acetabulum: what is normal? *Clin Orthop Relat Res.* 2009;467:868–875.
17. Liechti EF, Ferguson SJ, Tannast M. Protrusio acetabuli: joint loading with severe pincer impingement and its theoretical implications for surgical therapy. *J Orthop Res.* 2015;33:106–113.
18. Mavcic B, Igljic A, Kralj-Igljic V, Brand RA, Vengust R. Cumulative hip contact stress predicts osteoarthritis in DDH. *Clin Orthop Relat Res.* 2008;466:884–891.
19. Mechlenburg I, Nyengaard JR, Rømer L, Søballe K. Changes in load-bearing area after Ganz periacetabular osteotomy evaluated by multislice CT scanning and stereology. *Acta Orthop Scand.* 2004;75:147–153.
20. Michaeli DA, Murphy SB, Hipp JA. Comparison of predicted and measured contact pressures in normal and dysplastic hips. *Med Eng Phys.* 1997;19:180–186.
21. Murphy SB, Ganz R, Müller ME. The prognosis in untreated dysplasia of the hip. A study of radiographic factors that predict the outcome. *J Bone Joint Surg Am.* 1995;77:985–989.
22. Philippon MJ, Wolff AB, Briggs KK, Zehms CT, Kuppersmith DA. Acetabular rim reduction for the treatment of femoroacetabular impingement correlates with preoperative and postoperative center-edge angle. *Arthroscopy.* 2010;26:757–761.
23. Reynolds D, Lucas J, Klaue K. Retroversion of the acetabulum. A cause of hip pain. *J Bone Joint Surg Br.* 1999;81:281–288.
24. Rosset A, Spadola L, Ratib O. OsiriX: an open-source software for navigating in multidimensional DICOM images. *J Digit Imaging.* 2004;17:205–216.
25. Steppacher SD, Anwander H, Zurmühle CA, Tannast M, Siebenrock KA. Eighty percent of patients with surgical hip dislocation for femoroacetabular impingement have a good clinical result without osteoarthritis progression at 10 years. *Clin Orthop Relat Res.* 2015;473:1333–1341.
26. Steppacher SD, Huemmer C, Schwab JM, Tannast M, Siebenrock KA. Surgical hip dislocation for treatment of femoroacetabular impingement: factors predicting 5-year survivorship. *Clin Orthop Relat Res.* 2014;472:337–348.
27. Steppacher SD, Lerch TD, Gharanizadeh K, Liechti EF, Werlen SF, Puls M, Tannast M, Siebenrock KA. Size and shape of the lunare surface in different types of pincer impingement: theoretical implications for surgical therapy. *Osteoarthr Cartil.* 2014;22:951–958.
28. Tannast M, Goricki D, Beck M, Murphy SB, Siebenrock KA. Hip damage occurs at the zone of femoroacetabular impingement. *Clin Orthop Relat Res.* 2008;466:273–280.
29. Tannast M, Hanke MS, Zheng G, Steppacher SD, Siebenrock KA. What are the radiographic reference values for acetabular under- and overcoverage? *Clin Orthop Relat Res.* 2015;473:1234–1246.
30. Tönnis D, Heinecke A. Acetabular and femoral anteversion: relationship with osteoarthritis of the hip. *J Bone Joint Surg Am.* 1999;81:1747–1770.
31. Zhao X, Chosa E, Totoribe K, Deng G. Effect of periacetabular osteotomy for acetabular dysplasia clarified by three-dimensional finite element analysis. *J Orthop Sci.* 2010;15:632–640.